

1 **Accuracy of predicting chemical body composition of growing pigs using dual-**
2 **energy X-ray absorptiometry**

3 C. Kasper ^a, P. Schlegel ^a, I. Ruiz-Ascacibar ^{a,1}, P. Stoll ^a and G. Bee ^a

4

5 ^a *Swine Research Unit, Agroscope, Tioleyre 4, 1725 Posieux, Switzerland*

6 ¹ *Present address: Yara Iberian S.A.U., Infanta Mercedes St., E-28020 Madrid, Spain*

7

8 Corresponding author: Claudia Kasper. Email: claudia.kasper@agroscope.admin.ch

9

10 Short title: Body composition in pigs by DXA

11

12

13 **Abstract**

14 Studies in animal science assessing nutrient and energy efficiency or determining
15 nutrient requirements necessitate gathering exact measurements of body composition
16 or body nutrient contents. Wet chemical analysis methods or standardized dissection
17 are commonly applied, but both are destructive. Harnessing human medical imaging
18 techniques for animal science can enable repeated measurements of individuals over
19 time and reduce the number of individuals required for research. Dual-energy X-ray
20 absorptiometry (DXA) is particularly promising due to its low acquisition and operating
21 costs, low levels of radiation emission and simple image processing. However, the
22 measurements obtained with DXA do not perfectly match dissections or chemical
23 analyses, requiring the adjustment of the DXA via calibration equations. In principle,
24 DXA results should be independent of animal size and body composition, because
25 bone mineral content and the content of fat and lean tissue are derived from the
26 attenuation of X-rays transmitted through the body. Several calibration regressions
27 have been published, but comparative studies are pending. Thus, it is currently not
28 clear whether existing regression equations can be directly used to convert DXA
29 measurements into chemical values or whether each individual DXA device will require
30 its own calibration for the animal's breed, age, class or sex. Our study builds prediction
31 equations that relate body composition to the content of single nutrients in growing
32 entire male pigs (body weight range 20–100 kg) as determined by both DXA and
33 chemical analyses, and we present the accuracy of those predictions. Moreover, we
34 show that the chemical composition of the empty body can be satisfactorily determined
35 by DXA scans of carcasses. This opens up promising possibilities for the reduction of
36 invasive procedures in the course of nutritional studies. Finally, we compare existing
37 prediction equations for pigs of a similar range of body weights with the equations

38 derived from our DXA measurements and evaluate their fit with our chemical analyses
39 data. We found that existing equations for absolute contents that were built using the
40 same DXA beam technology predicted our data more precisely than equations based
41 on different technologies and percentages of fat and lean mass. This indicates that the
42 creation of generic regression equations that yield reliable estimates of body
43 composition in pigs of different growth stages, sexes and genetic breeds could be
44 achievable in the near future. DXA may be a promising tool for high-throughput
45 phenotyping for genetic studies, because it efficiently measures body composition in a
46 large number and wide array of animals.

47
48 **Keywords:** swine, bone mineral content, DXA, calibration, imaging techniques
49

50 **Implications**

51 The ability to determine body composition non-invasively opens opportunities for
52 improving studies of nutrition, nutrient balance and genetics. The present study
53 contains regression equations to estimate the nutrient composition, such as energy,
54 water, bone minerals (ash), total calcium, total phosphorus, total crude protein, total
55 nitrogen and total lipids) in the empty body of live pigs and in pig carcasses within a
56 body-weight range from 20 to 100 kg using DXA. We present regression equations to
57 estimate the empty body composition directly from the carcass. This rapid and non-
58 destructive method permits to reduce costs, time and number of animals needed for
59 research, since the same individuals can be scanned repeatedly.

Deleted: (

Deleted: a

Deleted: P

Deleted: CP

Deleted: N

Deleted: BW

Deleted: EB

67 **Introduction**

68 For studies in animal science that include measurements of nutrient and energy
69 efficiency or the determination of protein, mineral and energy requirements, it is
70 necessary to determine exact body composition. Two destructive methods are
71 commonly used to determine body composition. Carcass dissection into fat, lean and
72 bone tissue is used to determine carcass quality for nutrition and genetic selection
73 studies. Wet chemistry analyses of the carcass are carried out to determine the nutrient
74 content, and thus the nutrient and energy deposition rate and efficiency. The latter
75 method certainly offers better accuracy and less operator bias, and it is commonly
76 considered the gold standard. But both techniques are destructive, expensive and
77 time-consuming, which precludes their application in studies requiring repeated
78 measurements on individuals or large samples sizes. However, assessment of body
79 composition or nutrient content *in vivo* could be used to evaluate the influence of
80 feeding strategies, housing systems or environmental factors on the development of
81 body composition or could facilitate monitoring nutrient efficiency. For genetics
82 research, determining body composition and nutrient content with non-destructive
83 methods could aid performance testing and the selection of parent individuals for
84 breeding. Therefore, harnessing medical imaging techniques originally designed for
85 humans, such as computed tomography (CT), magnetic resonance imaging (MRI) and
86 dual-energy X-ray absorptiometry (DXA), is a promising area for animal science
87 (Scholz et al., 2015). Imaging methods can be performed on carcasses or *in vivo* under
88 anaesthesia, which enables repeated measurements of individuals through time, and
89 can reduce the number of individuals required for research, as demanded by the 3R
90 principles (National Centre for the Replacement, Refinement and Reduction of Animals
91 in Research, 2019).

92
93 Medical imaging techniques such as DXA, CT and MRI not only enable repeated
94 measurements of the same individual but also yield more reproducible results than
95 dissections. Among medical imaging techniques, DXA has advantages that make it
96 particularly attractive for application in animal science (Pomar et al., 2017), which
97 mainly include financial and work security aspects. Compared to CT and MRI, DXA is
98 easier to use, has lower instrument and operating costs, a more rapid scan speed, little
99 to no operator bias and requires less image processing, consequently allowing for
100 quick data analyses (Scholz et al., 2015). Moreover, ionizing radiation emitted by DXA
101 is relatively low (Genton et al., 2002), making it a secure device for operators. The DXA
102 provides information about lean mass, fat tissue mass and bone mineral content
103 (BMC), the sum of which represents the total body mass. It also measures the bone
104 surface, allowing for determination of bone mineral density (BMC divided by bone
105 surface). However, because DXA is an indirect tool, it does not provide true values,
106 although its values are precise and have, for example, less incidence of random error
107 (Kipper et al., 2019a). Thus, the information from DXA devices does not fully
108 correspond with the data from invasive techniques, and it is therefore necessary to
109 adjust measurements to reference dissections or, ideally, chemical analyses via
110 prediction equations (Mitchell et al., 1998b). Regression equations have been
111 published for a range of breeds, sexes and weight classes of pigs, using different DXA
112 beam technologies (Mitchell et al., 1998a; Mitchell et al., 1998c; Pomar et al., 2001;
113 Mitchell et al., 2003; Suster et al., 2003; Pomar et al., 2017; Kipper et al., 2019b). The
114 image-processing software on DXA devices used to compute tissue masses was
115 developed for the human body. It is optimized for scanning humans in a supine
116 position, and it might rely on human-specific assumptions about the distribution of fat,

Deleted: primarily aspects related to financial and work security.

Deleted: 1998b

120 lean tissue and bone tissue (Genton et al., 2002; Hunter et al., 2011). Moreover,
121 because algorithms are proprietary, these assumptions cannot be checked or adapted
122 to animal species.

123
124 The results of imaging techniques should, in principle, be independent of animal size
125 and body composition, and therefore, regression equations might not require
126 adjustment for different growth stages, sexes and genetic breeds (Mitchell et al.,
127 1998a; Marcoux et al., 2005; Soladoye et al., 2016). To date, no comparative study
128 has evaluated the fit of previously published regression equations to a new set of data.
129 Thus, it is unclear whether existing regression equations can be directly used to
130 convert DXA measurements into chemical values or whether each individual DXA
131 device requires its own calibration. The objectives of this study on pigs of 20 to 100 kg
132 were 1) to estimate the chemical composition of the EB from values determined by
133 DXA on the live animal; 2) to estimate the chemical composition of the carcass from
134 the values determined by DXA on carcass; 3) to estimate the chemical composition of
135 the EB from the carcass values determined by DXA, over the complete range of body
136 weights. Finally, we compared existing prediction equations with the equations derived
137 from our data and evaluated their fit with our data.

138 **Materials and methods**

139 ***Animals***

140 We used 68 entire males originating from 17 litters in two farrowing series of the
141 Agroscope Large White pig dam line. The details of housing, feeding and slaughter
142 procedures were the same as described by Ruiz-Ascacibar et al. (2017). In brief, pigs
143 with a mean BW of 8.9 kg (\pm 2.1 kg SD) were selected at weaning and kept in

144 17.35 m² pens in groups of a maximum of 14. The pigs had *ad libitum* access to a diet
145 based on BW, with the pigs having < 20 kg BW receiving a weaning diet, those between
146 20 and 60 kg BW getting one of two grower diets and pigs with > 60 kg BW (20–60 kg
147 BW) being fed one of two finisher diets. The grower and finisher diets differed by 20%
148 in their CP content (165 vs 139 g CP per kg grower diet and 140 vs 117 g CP per kg
149 finisher diet). Both diets were formulated to contain the same amount of digestible
150 energy (13.2 MJ/kg feed). Pigs were either slaughtered at a live BW of 20 kg (*N* = 6)
151 or kept on feed until they reached a target BW of 60 kg (*N* = 18) or 100 kg (*N* = 37 for
152 EB, and *N* = 44 for carcass), as determined by weekly weighing (Grüter SST-WA-03,
153 Eschenbach, Switzerland; ± 100 g). Three days prior to slaughter (-3), the pigs were
154 fasted for at least 16h and then sedated using isoflurane (Attane, Piramal Critical Care,
155 Inc., Bethlehem, PA, USA) prior to DXA scanning. Sedation was conducted to prevent
156 movement during the scanning procedure. The pigs were scanned on the DXA and
157 subsequently their BW was determined using a scale (BW₋₃). The awakened pigs were
158 brought back to their respective pens. The live DXA scans under anaesthesia were
159 carried out three days before slaughter in order to meet the required withdrawal period
160 for isoflurane before the sale of carcasses for human consumption. A technical
161 problem occurred on the DXA that disabled scanning for a period of two weeks. Thus,
162 live scans of seven 100 kg category pigs could not be conducted. After 16 h of feed
163 withdrawal, the pigs were slaughtered using the Agroscope experimental abattoir for
164 exsanguination after CO₂ stunning. Pigs were weighed (Berkel IWS IT 6000, Berkel-
165 Obrecht, Spreitenbach, Switzerland; ±200 g) before and after exsanguination to
166 determine blood mass. The BW prior to exsanguination corresponds to the BW at
167 slaughter (BW_{slaughter}). Immediately after exsanguination, hair and claws were removed
168 and collected. Animals were then eviscerated and the carcass and head were sawed

169 into two halves. The two half carcasses including the head without brain were weighed
170 for correspondence with the warm carcass weight. Then, they were chilled at 2°C and
171 a cold carcass weight was determined 24 h *post mortem*. The left carcass halves
172 (including halved head without brain) were then processed into primal cuts (head,
173 neck, shoulder, ham, loin, tail and feet) and scanned using DXA. Subsequently, the
174 cuts were frozen for further processing to determine the carcass chemical composition
175 as described by Ruiz-Ascacibar et al. (2017). To prevent thawing and re-freezing, the
176 carcass halves were divided into primal cuts before scanning because grinding prior
177 to chemical analysis is always performed in a frozen state. The carcass cuts of the
178 seven pigs slaughtered during the DXA failure were exceptions in being thawed for the
179 DXA scanning and then re-frozen. The gall bladder, bladder, stomach, intestine and
180 hind gut were emptied and rinsed with clean water to remove any remaining bile, urine
181 and digesta. The eviscerated organs and brain were then pooled and homogenized for
182 further processing in order to determine the chemical composition of the EB as
183 described by Ruiz-Ascacibar et al. (2017).

184 *DXA image acquisition*

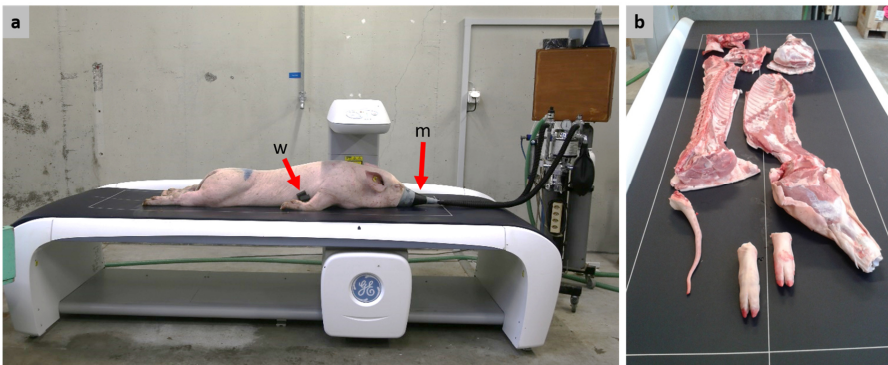
185 A GE Lunar DXA (~~i-DXA, GE Healthcare Switzerland, Glattbrugg, Switzerland~~) with a
186 narrow-angle fan beam (Collimator Model 42129) was used to scan the live pigs and
187 carcass halves. The DXA has a 100 kV generator and K-edge filtering, resulting in
188 approximately 39 keV and 71 keV X-ray effective energies. The calibration was
189 checked and passed before each scanning session by scanning a calibration phantom
190 according to the manufacturer's instructions. Scans were conducted using the 'total
191 body thick' mode (0.188 mA, scan speed 80mm/s according to Carver et al., 2013)
192 with enCORE software (version 16). It has to be noted that, according to the
193 manufacturer, this mode is not recommended for pigs of smaller sizes. In this study,

Deleted: i

Deleted: Chicago, IL, USA

Deleted: 100 kV,

197 the mode with the highest level of radiation was used for all individuals regardless of
198 size. This was done in order to avoid switching between modes, which could introduce
199 additional variation between the measurements of pigs of different BW classes. The
200 sedated pigs were placed on the DXA table in a standardized way in a prone position
201 with the hind legs extended while the front legs were positioned along the side but kept
202 away from the body by two wedges of foam plastic (Figure 1a). The left carcass cuts
203 were placed next to each other on the DXA table with the skin side facing downwards.
204 The cuts were arranged in a standardized manner to reflect an uncut half carcass
205 (Figure 1b). All scans started from the head.



206
207 **Figure 1 (a)** Positioning of live animals on the DXA table for scanning under anaesthesia. **w:** Plastic
208 foam wedge used to keep the front legs away from the body. **m:** Mask for the continuous
209 administration of isoflurane. **(b)** Positioning of cut carcass on the DXA table.
210

211 **DXA image processing**

212 Scan images from live animals were processed to remove artefacts (i.e. regions not
213 belonging to the animal, such as the mask and tube on the sedating apparatus and the
214 ear tag) and to position the regions of interest (ROI). The ROI were placed in order to
215 be similar to the human ROI according to the supplier's guidelines. This was done by
216 defining reference points for the pig (Supplementary Material Section 1, Figure S1).
217 The ROI in the scans of carcasses were set on "right arm" for all primal cuts. The

Deleted: according to manufacturer's recommendations.
Deleted: regions of interest
Deleted: placed so that they each contained one primal cut.

223 variables 'total mass', 'BMC' (bone mineral content), 'lean' and 'fat' of the live whole
224 body and of each left carcass half (listed in the upper part of Table 1) were exported
225 from the software and used for further analysis.

226 **Laboratory analyses and calculations**

227 Chemical analyses of energy, water, ash, Ca, P, N and lipid content (listed in the lower
228 part of Table 1) were conducted as described in Ruiz-Ascacibar et al. (2017; 2019). In
229 brief, all fractions of the EB_{slaughter}, which were 1) the pooled left carcass cuts, including
230 the left half of the head without brain, 2) the pooled empty digestive tract, the organs
231 and brain, 3) the hair and claws and 4) the blood, were ground, homogenised and dried
232 separately. For the EB_{slaughter}, all calculations of contents were based on warm carcass
233 weight (to closely mimic the situation in the live animal), and for the carcass, they were
234 based on cold carcass weight. The contents of energy, water, ash, Ca, P, N and lipids
235 in the left carcass half were combined with those of the right carcass half to obtain
236 values for the full carcass. The CP content was calculated by multiplying the N content
237 determined by wet chemistry by 6.25. Analyses were conducted in duplicate, but if
238 results differed by more than 5%, up to four replicates were analysed. Since the live
239 pigs were scanned by DXA three days prior to slaughter, the chemical composition of
240 the EB at that time (EB₋₃) was obtained individually from the EB_{slaughter} values as
241 follows: The chemical composition of EB_{slaughter} was divided by EBW_{slaughter} and
242 multiplied by EBW₋₃. The EBW₋₃ corresponded to the BW₋₃ multiplied by 95.3%, 96.2%
243 or 95.6% (the average ratio of EBW slaughter to BW slaughter for the 20, 60 and 100
244 kg category pigs, respectively).

245

246 *Statistical analysis of results*

247 The plausibility of the data was checked before the statistical analysis (Supplementary
248 Material Section 2), including a check of the differences between the total levels of raw
249 ash, CP, lipids and water and the EBW_{slaughter} and cold carcass weight obtained by
250 scales. Histograms of the raw data obtained by chemical analyses (Figure S2) were
251 visually checked. In all analyses, the experimental unit was the individual pig. The code
252 on which statistical analyses were based in R (version 3.6.3; R Core Team, 2020) can
253 be found in the Supplementary Material. For the comparison of chemical and DXA-
254 derived values, we conducted Welch's two-sample t-test for unequal variances. To
255 compute the difference, we subtracted the mean of the respective chemical value from
256 the DXA value and expressed it as a percentage of the chemical value. Regression
257 equations were computed with the lm() command, and figures were created using the
258 package ggplot2 (version 3.2.1; Wickham, 2016). BW_{DXA}, energy_{DXA}, water_{DXA}, ash_{DXA},
259 Ca_{DXA}, P_{DXA}, CP_{DXA}, N_{DXA} and lipid_{DXA} were used to denote the values predicted by the
260 regression equations. To facilitate interpretation, we kept variables on their original
261 scale in all models. The models for predicting EBW₋₃ and carcass weight contained
262 total mass by DXA as the sole predictor variable. A stepwise reduction of linear models
263 was used to select estimates of body composition provided by DXA. The full models
264 for the prediction of all chemical parameters included BMC, lean tissue and fat tissue
265 as estimated by DXA. In case more than one of the predictors of the full model was not
266 significant, we first omitted the variable from which, from a biological point of view, we
267 expected the weakest relationship to the estimated chemical content. Because the
268 data stem from an experiment with different dietary treatments, we examined whether
269 dietary treatment had an effect on the slopes and intercepts of the regression equations
270 (Supplementary Material Section 3). The effect of dietary treatment was never

Deleted: 1

Deleted: 1

Deleted: 2

274 significant and the inclusion of the dietary treatment changed slopes and intercepts
275 only marginally (Table S1); thus, we present models without dietary treatments.
276 Adjusted R^2 as a measure of goodness-of-fit was extracted from the R model object,
277 and the root mean square error (RMSE) was calculated as $\sqrt{\frac{\sum_{i=1}^n (\text{measured} - \text{predicted})^2}{n}}$,
278 where *measured* is the value determined by chemical analysis, *predicted* is the value
279 estimated from the DXA measurement via the regression equation and *n* is the sample
280 size. To facilitate comparison among variables with a wide range of contents in the
281 body, we computed the residual coefficient of variation (rCV), which is the percentage
282 of the RMSE to the chemically measured value, as a standardized metric. We
283 performed cross-validation of the regression equations via a jack-knife approach by
284 iteratively omitting one data point from the data set and computing the prediction error,
285 using the leave-one-out method in the caret package (version 6.0-86; Kuhn, 2020).
286 The models did not fully comply with the assumptions for linear least squares
287 regressions (Supplementary Material Section 4), which could possibly lead to a
288 misestimation of the parameters. Thus, using the leave-one-out cross-validation
289 procedure, we checked whether the estimates of intercepts and slopes were robust or
290 if they deviated from our estimates due to a disproportionate leverage of certain data
291 points. This also allowed us to derive non-parametric confidence intervals for slopes
292 and intercepts (for details, see Supplementary Material Section 4). Even though our
293 main goal was to build regression equations over the whole range of slaughter weights,
294 we also present specific (regional) regressions for each target slaughter-weight
295 category (20, 60 and 100 kg, see Supplementary Material Section 5). This was done
296 to compare the slopes and intercepts of regional regressions with the ones of the global
297 regression. However, these are probably less reliable since they are based on only a

Deleted: jackknife

Deleted: 3

Deleted: 3

301 subset of the data, and the number of observations for each regression is low, in
302 particular for the 20 kg category.

303
304 Finally, we compared the prediction equations we obtained from our data set with those
305 published in the literature (Mitchell et al., 1998a; Mitchell et al., 1998c; Pomar et al.,
306 2001; Mitchell et al., 2003; Pomar et al., 2017; Kipper et al., 2019b). To do this, we
307 applied the published equation to the DXA values of our data set and computed the
308 RMSE of the values predicted using the published equations and the chemically
309 measured values from our study.

310 **Results and discussion**

311 *Correspondence of wet chemistry and DXA measurements*

312 Table 1 shows the descriptive statistics of DXA values from the live pigs three days
313 prior to slaughter and from the carcass, the scale weight of the EB-3 and carcass and
314 the wet-chemistry values from the EB-3 and the carcass, respectively. Table 2 shows
315 the results of testing for significant differences between DXA and chemical values.
316 Scale weight and DXA weights of the EB and carcass were comparable ($P > 0.05$),
317 with a mean difference of 1% in both EB and carcass. As noted previously, the exact
318 correspondence of body weight measured by DXA and weigh scales does not
319 necessarily mean that the body composition determined by the two measuring
320 methods is equally accurate (Mitchell et al., 1998c). In contrast to body weight, the
321 values for ash, CP and lipids obtained from chemical analyses differed ($P < 0.01$) from
322 the BMC, lean tissue and fat mass obtained by DXA, except for the values of lipids and
323 fat in the carcass ($P > 0.05$). Such observations were reported previously (Suster et
324 al., 2003). The DXA readout does not provide information on water content. Therefore,

Deleted: 1998b

Deleted: By

327 the water content in the fat-free mass (sum of CP, ash and water), which was
328 determined by chemical methods, must be taken into account. It represented 76% (\pm
329 1.46% SD; CV=1.91%) in the EB and 74% (\pm 1.47% SD; CV=2.00%) in the carcass.
330 This content is in line with the reported 73% to 77% water in fat-free mass (Speakman,
331 1997; Bocquier et al., 1999; Lerch et al., 2015). Because the major proportion of body
332 water is in the fat-free mass and because DXA derives lean tissue mass indirectly via
333 body water (Hunter et al., 2011), the water may be attributed with CP to DXA lean. The
334 sum of CP and water mass was comparable ($P > 0.05$) with lean mass. The higher
335 concordance between lean mass and CP with water in the carcass in comparison to
336 the EB could be explained by gut water content and/or a lipid-to-protein ratio in the
337 intestines and organs that differs from that in the carcass.

338
339 The BMC was 34% and 21% lower ($P < 0.01$) than the ash content of the EB and
340 carcass, respectively. The skeleton is rich in minerals and contains a high proportion
341 of certain minerals, such as Ca and P. However, other minerals found in body ash are
342 mainly present in body tissues and fluids, so they are not considered as part of BMC.
343 Thus, BMC is expected to be lower than body ash. When comparing BMC with ash in
344 single bones, the correspondence of the values was greatly improved (Schlegel and
345 Gutzwiller, 2020). Fat tissue mass was 24% lower ($P < 0.05$) than lipid content in the
346 EB but comparable ($P > 0.05$) in the carcass. The fat content of the gastrointestinal
347 tract, the organs and the visceral adipose tissue (see Weigand et al., 2020) may have
348 caused this discrepancy.

349 Table 1. Body and carcass composition of growing pigs determined at 20, 60 and 100 kg body weight

	BW category	Empty body				Total carcass				
		Mean	SD	Min ^a	Max ^b	Mean	SD	Min ^a	Max ^b	
DXA	Total mass (g)	20	18756	884	17819	20350	13438	808	12667	14981
		60	57979	2410	54005	62604	44229	2178	40386	49095
		100	99963	3437	92085	106175	75916	2614	70892	81680
	BMC ^c (g)	20	414	12	395	427	450	21	420	474
		60	1378	94	1194	1569	1497	109	1279	1696
		100	2357	222	1874	2790	2522	265	1895	3057
	Lean (g)	20	16957	781	16083	18365	11535	691	10828	12725
		60	50452	2219	47393	54702	35904	2003	32395	39253
		100	84050	3836	78359	91771	59948	2707	54925	67860
Fat (g)	20	1384	133	1216	1558	1454	294	991	1786	
	60	6149	804	4991	7876	6828	920	4939	8793	
	100	13556	2134	9013	16746	13446	2000	9087	17357	
EBW ₃ or carcass weight (g)	20	18400	876	17500	20000	13520	800	12809	15055	
	60	57117	2320	53250	61600	43971	2144	40225	48886	
	100	98619	3391	90650	104800	75409	2551	70474	81081	
Energy content (MJ)	20	120	12	108	141	105	13	94	128	
	60	535	38	479	627	476	39	420	576	
	100	1028	78	858	1192	899	69	752	1048	
Water (g)	20	12761	504	12182	13664	9333	455	8882	10160	
	60	35737	1628	33925	39583	26909	1343	24533	29328	
	100	58585	2762	54251	64877	44203	2066	40703	50787	
Wet Chemistry	Ash (g)	20	556	36	488	586	542	40	473	583
		60	1844	130	1562	2066	1799	137	1538	1987
		100	3156	469	2043	4261	3054	451	1941	4118
	Calcium (g)	20	156	13	137	172	166	15	147	186
		60	564	68	463	755	582	70	475	766
		100	955	179	477	1397	974	175	487	1413
	Phosphorus (g)	20	95	10	77	103	94	10	76	103
		60	317	33	272	402	313	35	258	394
		100	545	75	345	715	532	75	333	701
	CP (N×6.25, g)	20	2709	104	2585	2880	2200	114	2084	2409
		60	9264	644	8231	10343	7745	644	6742	9003
		100	16079	909	14210	18218	13279	844	11487	15595
Nitrogen (g)	20	433	17	414	461	352	18	333	385	
	60	1482	103	1317	1655	1239	103	1079	1440	
	100	2573	145	2274	2915	2125	135	1838	2495	
Lipids (g)	20	1454	245	1170	1829	1394	255	1132	1806	
	60	8142	989	5951	10226	7554	972	5486	9768	
	100	16567	2269	10910	20750	14964	2013	10016	18912	

Deleted: /

350 ^aMinimum
 351 ^bMaximum
 352 ^cBone mineral content

354 **Table 2** Means and standard deviations of variables measured by DXA and determined by chemical
 355 analyses (or scales) and the results of Welch's two-sample t-test comparing DXA and chemical values
 356 in growing pigs

	Item DXA	Item Chemical	DXA [g]	Chemical [g]	$\Delta\%$ ^a	t ^b	df	P
Empty Body	Total mass	EBW ₃	79587 ± 27838	78482 ± 27504	1	0.22	119.98	0.826
	BMC ^c	Ash	1877 ± 680	2513 ± 954	-34	-4.22	108.47	<0.001
	Lean	CP	67537 ± 22844	12753 ± 4602	81	18.36	64.86	<0.001
	Lean	CP + water	67537 ± 22844	60089 ± 20181	11	1.91	118.20	0.059
	Fat	Lipid	10173 ± 4749	12594 ± 5609	-24	-2.57	116.83	0.011
Carcass	Total mass	Carcass weight	62016 ± 20708	61626 ± 20521	1	0.11	133.99	0.913
	BMC ^c	Ash	2068 ± 711	2500 ± 901	-21	-3.1	127.11	0.002
	Lean	CP	49312 ± 16005	10836 ± 3705	78	19.31	74.16	<0.001
	Lean	CP + water	49312 ± 16005	47385 ± 15215	4	0.72	133.66	0.473
	Fat	Lipid	10636 ± 4407	11806 ± 4895	-11	-1.46	132.55	0.146

357 ^aDifference between DXA and chemical values as a percentage of chemical value

358 ^bStatistic from Welch's two-sample t-test

359 ^cBone mineral content

360

361 Given the expected discrepancies between the values obtained by DXA and wet
 362 chemistry, the conversion of DXA estimates of body composition via prediction
 363 equations was necessary to obtain quantitative estimates of body composition. The
 364 prediction equations had similar high precision and accuracy for EB and carcass. The
 365 non-parametric confidence intervals show that estimates of slopes and intercepts were
 366 robust (Table 3) even though model diagnostics were not optimal (see Supplementary
 367 Material Section 4).

Deleted: 3

368

369 *Weight*

370 The EBW and carcass weight could be predicted by the regression equations using
 371 DXA total mass with the highest R^2 and lowest rCV (Table 3, Figure 2, Figure 3). This
 372 was expected given the non-significant difference between the weights obtained by
 373 scales and DXA (Table 2). The RMSEs in the EB and the carcass were very similar,
 374 and we obtained an excellent fit ($R^2 = 1$ after rounding) with both EB and carcass. The
 375 intercept of the prediction equation was slightly shifted below zero for the EB, and
 376 above zero for the carcass. The slope was almost 1 in the EB and slightly below 1 in

378 the carcass. This shows that DXA can estimate the BW with very high reliability. The
379 coefficients of regional regressions for each target slaughter-weight category were very
380 similar to the global regression and all obtained very high R^2 (Table S2, Figures S3
381 and S4).

382

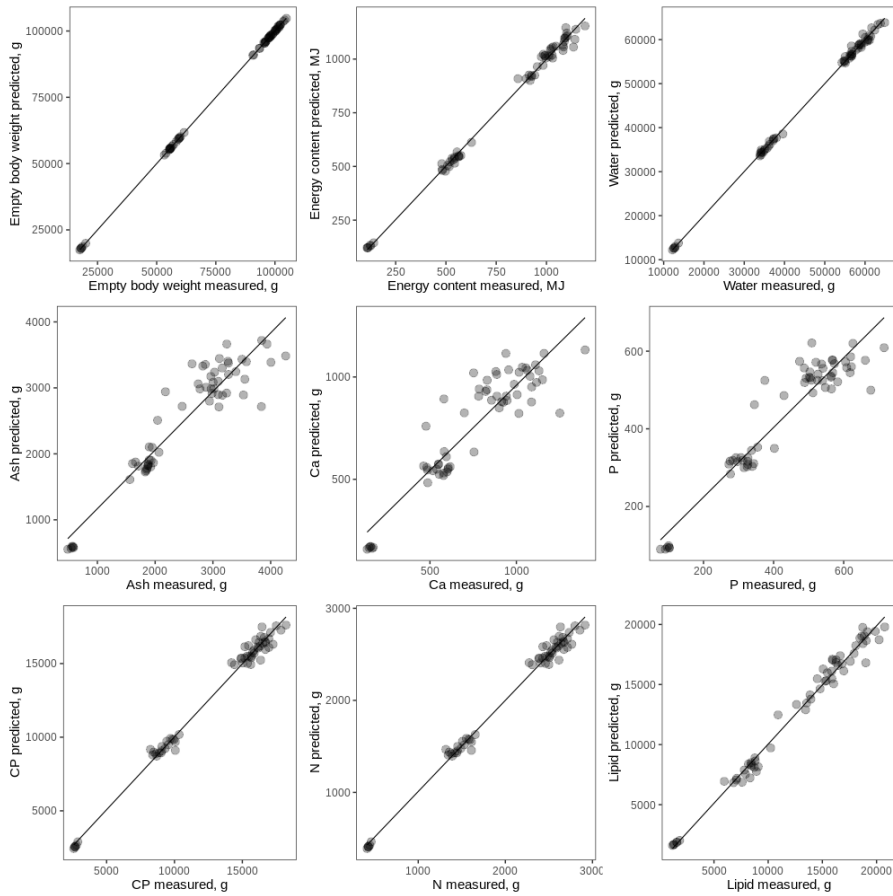
383 *CP, N, water and lipids*

384 For energy_{DXA}, CP_{DXA}, N_{DXA} and water_{DXA}, we obtained excellent precision and
385 accuracy in terms of R^2 (> 0.99) (Figure 2 and 3) and error (rCV $< 3.6\%$) when we
386 back-predicted the chemical values using the equations presented in Table 3. Lipid_{DXA}
387 was slightly less precise ($R^2 > 0.97$). Accuracy was better in the EB than in the carcass
388 (rCV = 5.4% and 7%, respectively). The DXA values for fat were consistently lower
389 than chemically measured lipid values for the pigs in the 20-kg slaughter category,
390 which was more pronounced in the empty body than in the carcass. The same
391 phenomenon was observed in a study comparing DXA and chemical analyses in small
392 pigs (5 to 27 kg live weight; (Mitchell et al., 1998b)). It appears that DXA overestimates
393 the fat content of pigs with a high percentage of body fat ($> 20\%$) and underestimates
394 the fat content in lean pigs (Mitchell et al., 1998b). Similar findings have also been
395 reported in humans (Genton et al., 2006). Because CP in the present study was directly
396 calculated from N, the precision and error of the prediction equations for N_{DXA} are
397 analogous to the ones for CP_{DXA} from lean mass. The ease with which we could predict
398 water content from lean tissue by DXA (water_{DXA}) can be related to the fact that lean
399 tissue mass is not measured directly by DXA but is instead derived from the water
400 content and is based on specific assumptions, such as a fixed ratio of lean tissue mass
401 to water content (Hunter et al., 2011; but note that they used a different DXA device
402 and software). Regional regression lines overlapped with the global one and obtained

403 similar R^2 and error, except for CP and N, which had reduced R^2 (Table S2, Figures
404 S3 and S4).

405
406 *Minerals*

407 Predictions of ash_{DXA}, Ca_{DXA} and P_{DXA} were less precise (R^2 between 0.80 and 0.89)
408 and subject to major error (rCV between 12.0 and 16.5%; Table 3). Ca and P contents
409 are certainly strongly correlated with the ash content, and one must expect that these
410 predictions cannot be better than those of the ash content. Whereas Ca_{DXA} solely
411 depended on BMC, P_{DXA} also included lean mass, which is in line with the knowledge
412 that body Ca and P are found at about 99% and 80%, respectively, in the bones (Suttle,
413 2010). A similar lower prediction accuracy for ash has been reported in other studies
414 (Suster et al., 2003). The slopes of regional regressions for each target slaughter-
415 weight category differed importantly for ash and P, but were rather similar for Ca (Table
416 S2, Figures S3 and S4). Fitting regional regressions did not only result in reduced
417 prediction errors, but also reduced R^2 compared to the global regression. This
418 suggests that it is difficult to fit reliable regional calibration models for ash, Ca and P
419 with the present dataset, and that more data and more work is needed.



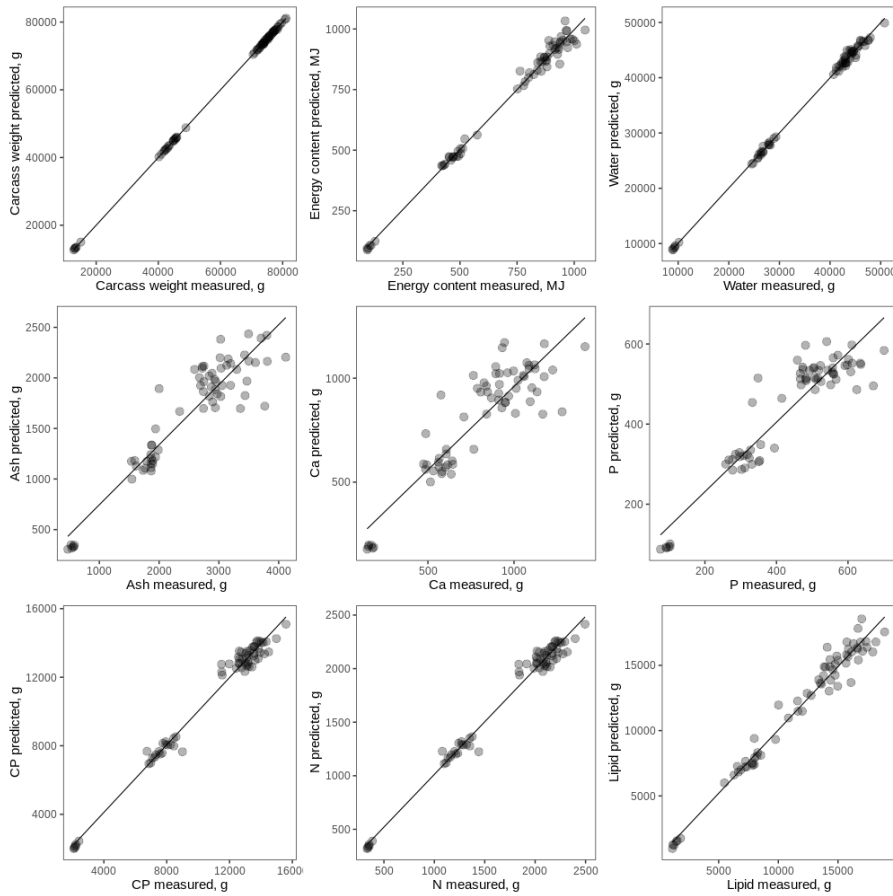
420

421 **Figure 2** Predicted values against measured chemical values in the empty body of growing pigs.
 422 Predicted values were obtained by applying the regression equations to the DXA measurements.
 423 Dots represent individual data points.

424

Deleted: Empty body regression equations of weight and chemical composition according to DXA values in growing pigs.

Deleted: For energy, the regression line for a reduced model including only total mass by DXA (instead of lean and fat from DXA) is shown. Also, for P and lipids, only the line of the reduced regression including BMC and fat by DXA, respectively, are shown.



434

435 **Figure 3** Predicted values against measured chemical values in the carcass of growing pigs.
 436 Predicted values were obtained by applying the regression equations to the DXA measurements. Dots
 437 represent individual data points.
 438

439

Deleted: Carcass regression equations of weight and chemical composition according to DXA values in growing pigs.

Deleted: For energy, the regression line for a reduced model including only total mass by DXA (instead of lean and fat from DXA) is shown. Also, for ash and P, only the lines of the reduced regressions including BMC by DXA are shown. Similarly, the regression line for lipid is the reduced regression including BMC fat from DXA.

450 *Prediction of empty body composition at slaughter from carcass*

451 The use of carcass DXA scans to predict the ash and CP content of the EB produced
452 levels of accuracy and low error that were equivalent to those obtained by predicting
453 EB ash and CP content from live scans (Table 3, Figure 4). The prediction of lipid
454 content of the EB using carcass fat content determined by DXA was marginally less
455 precise and had greater error ($R^2 = 0.96$ vs 0.97 , $rCV = 8.5\%$ vs 5.4%) than
456 predictions from live scans (Table 3, Figure 4). With increasing BW, the regression
457 line of the prediction models for CP_{DXA} in the EB based on carcass scans deviated
458 from those with the live scans. The reason for this might be that a considerable
459 amount of lipids and CP are contained in the organs and thus missing from the
460 carcass. Depending on the nature of the problem (e.g. when repeated measurements
461 are not necessary) and the required degree of accuracy and prediction, invasive
462 scanning of live animals requiring anaesthesia could, therefore, be replaced by
463 carcass scans.
464

465 **Table 3.** Models to estimate chemical composition of the empty body and the carcass from DXA values

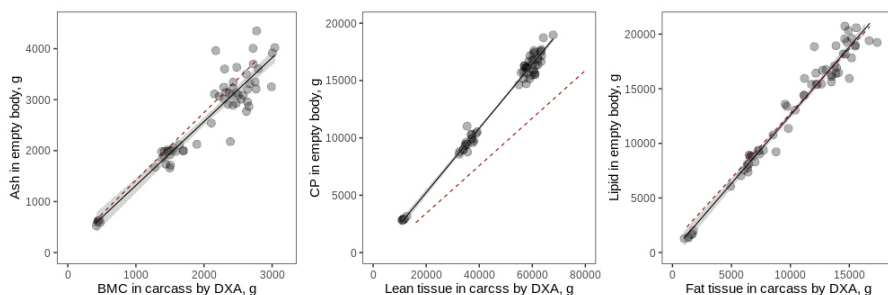
	Chemical variable (predicted variable)	Term (DXA variable)	Estimate ^a	P	R ²	RMSE ^b	rCV ^b
Empty body	Empty body weight (BW_{DXA})	Intercept	-149.059 (-157.219, -142.729)	0.015	1.000	150.08 <u>g</u>	0.20%
		Total mass	0.988 (0.988, 0.988)	< 0.001		154.12 <u>g</u>	0.20%
	Energy content (energy_{DXA})	Intercept	-34.94 (-35.915, -33.029)	0.001	0.995	22.90 <u>MJ</u>	2.90%
		Lean	0.007 (0.006, 0.007)	< 0.001		24.22 <u>MJ</u>	3.10%
		Fat	0.038 (0.037, 0.038)	< 0.001			
	Water (water_{DXA})	Intercept	1254.428 (1216.314, 1287.547)	< 0.001	0.999	578.90 <u>g</u>	1.20%
		Lean	0.682 (0.682, 0.683)	< 0.001		594.95 <u>g</u>	1.30%
	Ash (ash_{DXA})	Intercept	32.3 (18.894, 44.955)	0.792	0.886	316.73 <u>g</u>	12.60%
		BMC	1.322 (1.313, 1.333)	< 0.001		325.01 <u>g</u>	12.90%
	Ca (Ca_{DXA})	Intercept	-2.807 (-7.461, 1.962)	0.953	0.829	123.37 <u>g</u>	16.20%
		BMC	0.407 (0.404, 0.411)	< 0.001		126.50 <u>g</u>	16.60%
	P (P_{DXA})	Intercept	-9.819 (-12.744, -7.637)	0.653	0.893	52.20 <u>g</u>	12%
		BMC	0.145 (0.131, 0.156)	< 0.001		55.49 <u>g</u>	12.80%
		Lean	0.003 (0.002, 0.003)	0.033			
	CP (CP_{DXA})	Intercept	-784.767 (-805.418, -760.985)	< 0.001	0.99	454.08 <u>g</u>	3.60%
		Lean	0.2 (0.2, 0.201)	< 0.001		466.43 <u>g</u>	3.70%
N (N_{DXA})	Intercept	-125.563 (-128.867, -121.758)	< 0.001	0.99	72.65 <u>g</u>	3.60%	
	Lean	0.032 (0.032, 0.032)	< 0.001		74.63 <u>g</u>	3.70%	
Lipids (lipid_{DXA})	Intercept	-294.21 (-342.958, -230.694)	0.336	0.984	690.75 <u>g</u>	5.50%	
	Fat	0.986 (0.974, 0.996)	< 0.001		730.25 <u>g</u>	5.80%	
	Lean	0.042 (0.04, 0.045)	< 0.001				
Carcass	Carcass weight (BW_{DXA})	Intercept	172.744 (164.49, 180.989)	0.005	1.000	151.36 <u>g</u>	0.20%
		Total mass	0.991 (0.991, 0.991)	< 0.001		154.90 <u>g</u>	0.30%
	Energy content (energy_{DXA})	Intercept	-36.077 (-36.933, -34.427)	0.002	0.990	27.10 <u>MJ</u>	3.80%
		Lean	0.007 (0.007, 0.008)	< 0.001		28.57 <u>MJ</u>	4.00%
			0.036 (0.036, 0.037)	< 0.001			

		Fat					
Empty body from carcass	Water (water _{DXA})	Intercept	1058.187 (1037.353, 1083.199)	< 0.001	0.998	545.64 <u>g</u>	1.50%
		Lean	0.720 (0.719, 0.720)	< 0.001		558.48 <u>g</u>	1.50%
	Ash (ash _{DXA})	Intercept	-33.611 (-46.826, -19.201)	0.791	0.875	311.89 <u>g</u>	12.50%
		BMC	0.807 (0.766, 0.856)	< 0.001		325.87 <u>g</u>	13.00%
		Lean	0.018 (0.016, 0.019)	0.026			
	Ca (Ca _{DXA})	Intercept	19.401 (13.755, 25.059)	0.701	0.799	132.05 <u>g</u>	16.50%
		BMC	0.377 (0.374, 0.381)	< 0.001		135.06 <u>g</u>	16.90%
	P (P _{DXA})	Intercept	-6.388 (-9.128, -3.897)	0.781	0.863	56.53 <u>g</u>	13.00%
		BMC	0.109 (0.103, 0.121)	0.001		59.43 <u>g</u>	13.70%
		Lean	0.004 (0.004, 0.005)	0.002			
	CP (CP _{DXA})	Intercept	-482.745 (-500.385, -462.708)	0.014	0.983	476.85 <u>g</u>	4.40%
		Lean	0.230 (0.229, 0.230)	< 0.001		487.59 <u>g</u>	4.50%
	N (N _{DXA})	Intercept	-77.239 (-80.062, -74.033)	0.014	0.983	76.30 <u>g</u>	4.40%
		Lean	0.037 (0.037, 0.037)	< 0.001		78.01 <u>g</u>	4.50%
	Lipids (lipid _{DXA})	Intercept	-538.43 (-568.553, -483.998)	0.121	0.970	828.34 <u>g</u>	7.00%
		Fat	0.933 (0.916, 0.948)	< 0.001		870.83 <u>g</u>	7.40%
		Lean	0.049 (0.045, 0.052)	0.001			
	Empty body ash (ash _{DXA})	Intercept	65.76 (52.137, 79.908)	0.595	0.887	317.47 <u>g</u>	12.30%
		BMC carcass	1.252 (1.245, 1.263)	< 0.001		325.73 <u>g</u>	12.60%
	Empty body CP (CP _{DXA})	Intercept	-349.157 (-372.694, -321.981)	0.131	0.985	564.13 <u>g</u>	4.30%
		Lean carcass	0.28 (0.279, 0.28)	< 0.001		579.08 <u>g</u>	4.40%
	Empty body lipid (lipid _{DXA})	Intercept	-688.199 (-727.719, -628.837)	0.106	0.967	999.45 <u>g</u>	7.70%
		Fat carcass	1.067 (1.048, 1.088)	< 0.001		1058.83 <u>g</u>	8.20%
		Lean carcass	0.055 (0.05, 0.059)	0.004			

466 ^aIncluding their non-parametric confidence intervals, CI. For empty body: 93% CI, for carcass: 94% CI, empty body from carcass: 93% CI (see Supplementary
467 Material Section 4).

468 ^bNote: Upper value: RMSE and rCV from back-prediction of chemical values using the regression equations, lower value: RMSE and rCV from cross-
469 validation (leave-one-out method)

Deleted: 3



471

472 **Figure 4** Regressions of carcass DXA values (x-axis) on empty body chemical value (y-axis) in
 473 growing pigs. The red dashed lines are regression lines from corresponding prediction equations for
 474 live DXA scans on empty body values, as presented in Table 3. For lipids, the regression line for a
 475 reduced model including only fat by DXA (instead of fat and lean by DXA) is shown.

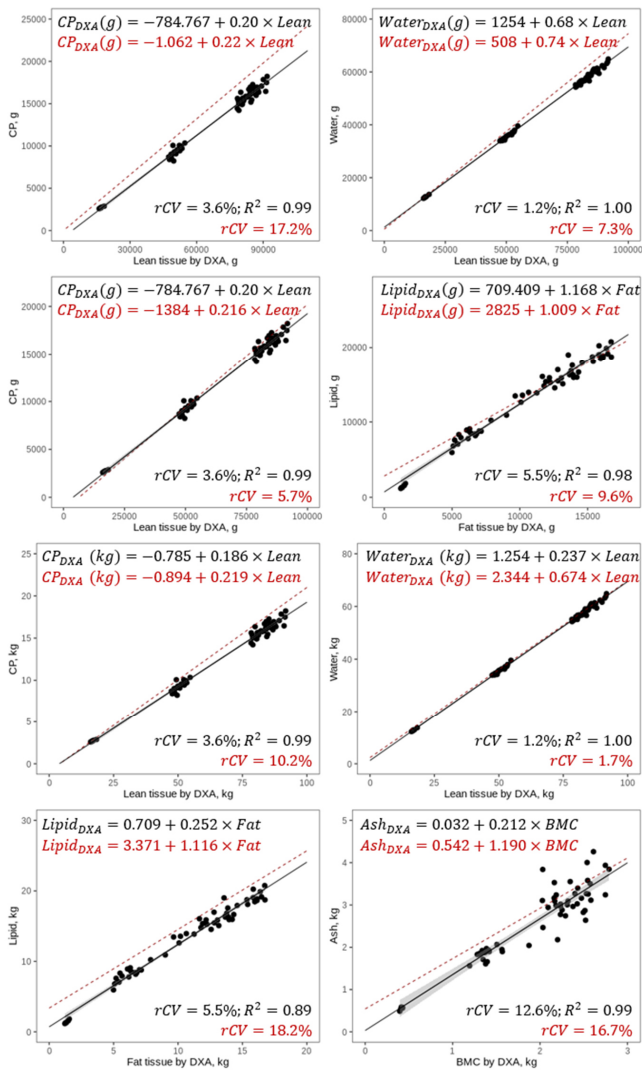
476 **Comparison with published regression equations**

477 *Empty body*

478 Our results are in line with published regression equations for the EB, which were built
 479 from wet chemistry analyses and live scans of pigs ranging from 5 to 97 kg live BW
 480 (Mitchell et al., 1998a), pigs with a mean live BW of 105.6 kg (Kipper et al., 2019b) and
 481 a mean warm carcass weight of 85 kg (Pomar et al., 2001, as cited in Pomar et al.,
 482 2017). Figure 5 shows the data points with regressions derived from this study and the
 483 regression lines from the literature for the EB (or live animal) for CP, water, fat and ash
 484 in the EB (or live animal). Concerning CP, the regression equations by Kipper et al.
 485 (2019b) (Figure 5, 2nd row) and Pomar et al. (2017) (Figure 5, 3rd row) fit our data quite
 486 well, whereas the one by Mitchell et al. (1998a) (Figure 5, 1st row) had a slightly worse
 487 fit. The intercepts of published equations and our study differ by 109 g to 784 g CP,
 488 which is a rather small amount given the total protein mass of the EB. Slopes were
 489 almost identical to our study (Figure 5). Using the regression by Mitchell et al. (1998a)
 490 to predict data from our study led to an overestimation of CP content in the EB
 491 throughout all weight categories. A possible explanation for the slightly worse fit of the
 492 regression equations from Mitchell et al. (1998a) than those from Kipper et al. (2019b)

493 and Pomar et al. (2017) could be the differences in the DXA technology used. As in
494 the present study, Kipper et al. (2019b) and Pomar et al. (2017) used a DXA scanner
495 with a narrow fan beam, whereas Mitchell et al. (1998a) used the pencil-beam
496 technology. It has been shown previously that different devices, and particularly
497 different beam technologies, yield considerably variable results in terms of total BW
498 (compared to scales), along with fat and lean mass in human subjects (Genton et al.,
499 2002) and livestock (Scholz et al., 2015). It is conceivable that in the case of extreme
500 proportions of body fat, such as, for example, piglets versus finishing pigs, or pigs
501 versus small ruminants or other livestock species, the absolute values obtained by
502 DXA could be inaccurate compared to the 'standard' body composition (Hunter et al.,
503 2011). The DXA technologies and their software might differ in the way they deal with
504 these issues, leading to the observed discrepancies. Concerning water, the published
505 equations from Mitchell et al. (1998a) (Figure 5, 1st row) and Kipper et al. (2019b)
506 (Figure 5, 3rd row) fit our data well (RMSE = 7.3% and 1.7%, respectively). The slopes
507 of the lines from the data in this study and from both published equations were similar.
508 Given the large amount of water in the body, differences in intercepts of approximately
509 776 g to 1 kg are not relevant, and the regression lines were very close to each other
510 (Figure 5). However, for pigs with higher BW, Mitchell's regressions led to a slight
511 overestimation of water content in the EB. Concerning lipids, the regression equation
512 by Pomar et al. (2017) had a relatively good fit to our data (Figure 5, 2nd row), with a
513 similar slope, and it differed by 2 kg at the intercept. Thus, while this regression
514 predicted the lipid content of pigs between 60–100 kg well, it overestimated the lipid
515 content of piglets. Regression equations for lipids and ash by Kipper et al. (2019b)
516 (Figure 5, 4th row) were similar to ours but consistently predicted higher values than
517 our equation did. Kipper et al.'s (2019b) slope for lipids was similar to ours; however,

518 their intercept was higher (by 2.7 kg), leading to a regression line almost parallel but
 519 slightly shifted upwards as compared to ours. Thus, using Kipper's equation on our
 520 data reflected well the differences between individuals in fat content by DXA, but it
 521 overestimated the actual values.



522
 523 **Figure 5** Comparison of own and published regression lines for DXA measurement on
 524 chemical value in empty body (live DXA scans) of growing pigs. The solid black lines are

525 regression lines obtained from the data in this study, and the dashed red lines are published
526 regression lines. Equations and rCV in black pertain to the present study; the equations in
527 red are previously published equations. rCV in red gives the prediction error of the published
528 equation applied to the DXA variable obtained in the present study. 1st row: lean tissue by
529 DXA on chemically determined CP and water in grams (Mitchell et al., 1998a). 2nd row: lean
530 and fat tissue by DXA on chemically determined CP and lipid in grams (Pomar et al., 2017).
531 3rd row: Lean tissue by DXA on chemically determined CP and lean tissue by DXA on
532 chemically determined water. 4th row: fat tissue by DXA on chemically determined lipids and
533 BMC by DXA on chemically determined ash in kilograms (Kipper et al., 2019b).
534

535 *Carcass*

536 The published equations for CP and water in half carcasses using absolute values
537 (Mitchell et al., [1998c](#)) built from wet chemistry analyses and carcass scans of pigs
538 slaughtered at a live BW of 30 to 120 kg fit our data well, with generally lower rCVs
539 than for the EB (Figure 6, upper row). The slopes were almost identical and the
540 intercepts differed by 640 g for CP and less than 400 g for water. Thus, the prediction
541 errors when using the equations by Mitchell et al. ([1998c](#)) were only slightly higher than
542 using our own regression equations. Comparing the regression equations for
543 percentages of lean mass and water with the ones from Mitchell et al. (2003), obtained
544 from half carcasses with a mean weight of 43 kg, proved to be more difficult. To create
545 our prediction equations, we calculated the percentage of lean tissue (sum of CP and
546 water) or fat in the carcass half as the proportion of the chemical value of the sum of
547 all chemical components (see Supplementary Material Section [6](#), Table [S3](#)). The
548 equations from Mitchell et al. (2003) were dramatically different from ours, with a
549 difference in the intercept of 13% for lean tissue and 33% for fat (Figure 6). The slopes
550 were also very different. The resulting regression lines clearly missed our data points.
551 This means that the equations published by Mitchell et al. (2003) are in no way suitable
552 for predicting the chemical values for the percentage of lean mass and lipid from the
553 present study. The reason for these striking differences could be that when the
554 absolute values are transformed to percentages, an important amount of variation and

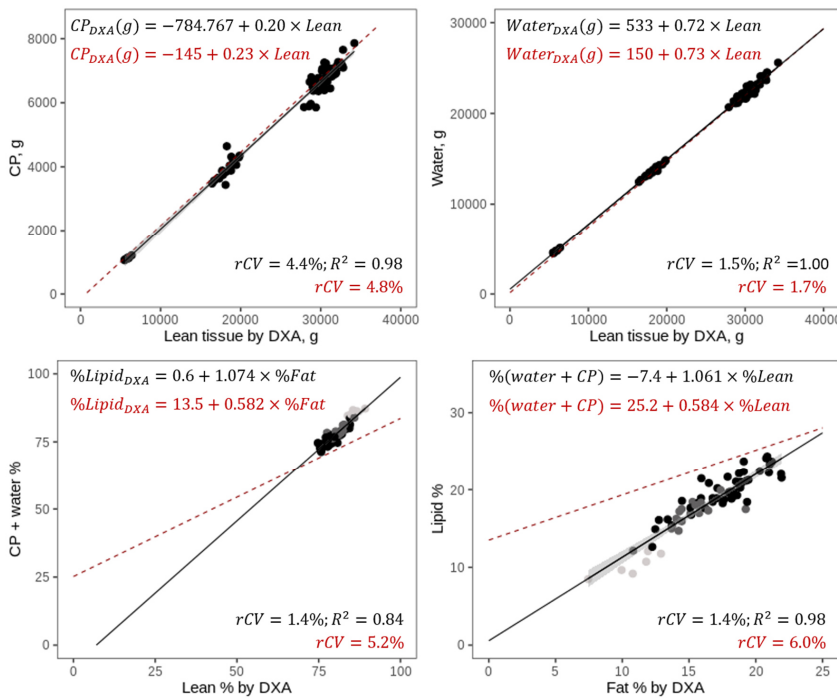
Deleted: 1998b

Deleted: 1998b

Deleted: 4

Deleted: S2

559 also co-variation between DXA and wet chemistry values is lost. Consequently, fitting
 560 a regression line through data points that have such a reduced variation is difficult, and
 561 the resulting parameters of the equations might not be as robust as the ones derived
 562 from regressions on the absolute values. The pigs in this study were within a rather
 563 narrow weight range (Mitchell et al., 2003), comparable to our 100 kg BW category.
 564 Thus, these equations might not be suitable for predicting the proportion of lean tissue
 565 and lipid in the smaller pigs in our study because those differ in the proportion of lean
 566 tissue and lipids from larger pigs (Figure 6 lower row). As for lipids, Mitchell et al.'s
 567 (2003) and our regression lines seemed to converge for pigs with a lipid content of
 568 around 30%, which was outside the range in our study.



569
 570 **Figure 6** Comparison of this study and other published regression lines for DXA
 571 measurement of chemical values in carcasses (live DXA scans) of growing pigs. Solid black
 572 lines are regression lines obtained from data in this study, while dashed red lines show
 573 published regression lines. Equations, rCV and R² in black pertain to the present study; the

574 equations in red are previously published equations. rCV in red gives the prediction error of
575 the published equation applied to the DXA variable obtained in the present study. Upper row:
576 lean tissue DXA on chemically determined CP and water in grams (Mitchell et al., 1998c).
577 Lower row: percentage of lean (CP + water) and fat tissue DXA on chemically determined
578 percentage of lean and fat mass (sum of EP and water; Mitchell et al., 2003). Different
579 categories of live weight at slaughter are illustrated by shading of the data points: light grey =
580 20 kg, dark grey = 60 kg, black = 100 kg.

Deleted: 1998b

581 **Conclusion**

582 In this work, we show that although calibration regressions are usually done for each
583 DXA device and/or working group, there is considerable agreement between the
584 parameters of published and our own regressions in pigs. Therefore, in the near future,
585 it might be quite realistic to create generic regression equations for body composition
586 in pigs that yield reliable estimates for pigs of different growth stages, sexes and
587 genetic breeds. To achieve this goal, all published results should ideally be
588 summarized within a meta-analysis or, even better, a joint analysis. This may allow for
589 a broader application of DXA, including for research groups that do not have the
590 possibility to generate their own calibration equations. This endeavour would be greatly
591 facilitated by data sharing among laboratories or, better, the existence of open data
592 sets providing both chemical and DXA values. We illustrate the possibility of predicting
593 the chemical content of individual nutrients such as P and Ca from DXA values. This
594 prospect is especially important for the emerging field of precision feeding, in which
595 the nutrient demands of single individuals have to be closely monitored. We have also
596 shown that body composition of the EB can be inferred with rather good precision and
597 accuracy from scanning carcass halves. Replacing the invasive, time-consuming and
598 labour-intensive scanning of live pigs with the scanning of carcasses has great
599 potential to improve animal welfare standards and could facilitate nutritional studies
600 that investigate overall nutrient deposition efficiency using a large number of animals.
601 Another promising application of DXA for measuring body composition in a relatively
602 efficient and low-cost manner are genetic studies. Currently, the effort associated with

604 chemical analysis certainly represents a bottleneck for those types of studies in which
605 traits have to be measured in hundreds to thousands of individuals. DXA could be
606 applied for high-throughput phenotyping, enabling the generation of large amounts of
607 data for many individuals.

608 **Ethics approval**

609 This experimental procedure was approved by the Office for Food Safety and
610 Veterinary Affairs (2015_37_FR) and all procedures were conducted in accordance
611 with the Ordinance on Animal Protection and the Ordinance on Animal
612 Experimentation.

613 **Data and model availability statement**

614 The data that support the findings of this study are publicly available in Zenodo
615 (Kasper *et al.*, 2020). The code used for models and the statistical analyses are listed
616 in the Supplementary Material (Section [Z](#)).

Deleted: 5

617 **Author ORCIDs**

618 C.K.: 0000-0001-7305-3996

619 P.S.: 0000-0001-5095-0889

620 G.B.: 0000-0002-6397-7543

621 **Author contributions**

622 Conceptualization: C.K. and P.S. Data Curation: C.K. and P.St. Formal Analysis:

623 C.K. Investigation: I.R.A., P.S., P.St. and G.B. Methodology: C.K., P.S. and G.B.

624 Software: C.K. and P.St. Supervision: P.S. and G.B. Visualization: C.K. Writing –

625 Original Draft Preparation: C.K. Writing – Review & Editing: C.K., P.S., I.R.A., P.St.

626 and G.B.

628 **Declaration of interest**

629 The authors report no conflicts of interest with any of the data presented.

630 **Acknowledgements**

631 We are grateful to Guy Maïkoff and his team for the maintenance and slaughter of
632 the pigs and assistance with carcass grinding and DXA scans, Sébastien Dubois and
633 his team for carrying out the chemical analyses and Andreas Gutzwiller for
634 assistance with DXA scans. We thank Armin Scholz and Candido Pomar for their
635 valuable technical advice concerning the performance of DXA scans on live pigs.

636 [Arthur Francisco Araujo Fernandes, Mathieu Monziols and an anonymous reviewer](#)
637 [provided valuable comments on a previous version of this manuscript.](#)

638 **Financial support statement**

639 This research received no specific grant from any funding agency, commercial or not-
640 for-profit.

641 **References**

- 642 Bocquier, F., Guillouet, P., Barillet, F. and Chilliard, Y., 1999. Comparison of three methods
643 for the in vivo estimation of body composition in dairy ewes. *Annales de Zootechnie* 48,
644 297–308.
- 645 Carver TE, Christou NV and Andersen RE 2013. In vivo precision of the GE iDXA for the
646 assessment of total body composition and fat distribution in severely obese patients.
647 *Obesity* 21, 1367–1369.
- 648 Genton, L., Hans, D., Kyle, U.G. and Pichard, C., 2002. Dual-energy X-ray absorptiometry
649 and body composition: Differences between devices and comparison with reference
650 methods. *Nutrition* 18, 66–70.
- 651 Genton L, Karsegard VL, Zawadynski S, Kyle UG, Pichard C, Golay A and Hans DB 2006.
652 Comparison of body weight and composition measured by two different dual energy X-

653 ray absorptiometry devices and three acquisition modes in obese women. *Clinical*
654 *Nutrition* 25, 428–437.

655 Hunter, T.E., Suster, D., Dunshea, F.R., Cummins, L.J., Egan, A.R. and Leury, B.J., 2011.
656 Dual energy X-ray absorptiometry (DXA) can be used to predict live animal and whole
657 carcass composition of sheep. *Small Ruminant Research* 100, 143–152.

658 Kasper, C., Schlegel, P., Ruiz-Ascacibar, I., Stoll, P. and Bee, G., 2020. Data of "Accuracy of
659 predicting chemical body composition of growing pigs by dual-energy X-ray
660 absorptiometry". Zenodo. DOI: 10.5281/zenodo.3981182.

661 Kipper, M., Marcoux, M., Andretta, I. and Pomar, C., 2019a. Assessing the accuracy of
662 measurements obtained by dual-energy X-ray absorptiometry on pig carcasses and
663 primal cuts. *Meat Science* 148, 79–87.

664 Kipper, M., Marcoux, M., Andretta, I. and Pomar, C., 2019b. Calibration of dual-energy x-ray
665 absorptiometry estimating pig body composition. In *Energy and protein metabolism and*
666 *nutrition, EAAP Scientific Series* (ed. G. Matteo Crowetto), pp. 427–429. Wageningen
667 Academic Publishers, Wageningen, The Netherlands.

668 Kuhn, M., 2020. caret: Classification and Regression Training. R package version 6.0-86.

669 Lerch, S., Lastel, M.L., Grandclaude, C., Brechet, C., Rycken, G. and Feidt, C., 2015. In
670 vivo prediction of goat kids body composition from the deuterium oxide dilution space
671 determined by isotope-ratio mass spectrometry. *Journal of Animal Science* 93, 4463–
672 4472.

673 Marcoux, M., Faucitano, L. and Pomar, C., 2005. The accuracy of predicting carcass
674 composition of three different pig genetic lines by dual-energy X-ray absorptiometry.
675 *Meat Science* 70, 655–663.

676 Mitchell, A.D., Scholz, A.M. and Conway, J.M., 1998a. Body composition analysis of pigs
677 from 5 to 97 kg by dual-energy X-ray absorptiometry. *Applied Radiation and Isotopes*
678 49, 521–523.

679 Mitchell AD, Scholz AM and Conway JM 1998b. Body composition analysis of small pigs by
680 dual-energy x-ray absorptiometry. *Journal of Animal Science* 76, 2392–2398.

681 Mitchell, A.D., Scholz, A.M. and Pursel, V.G., 2003. Prediction of pork carcass composition
682 based on cross-sectional region analysis of dual energy X-ray absorptiometry (DXA)
683 scans. *Meat Science* 63, 265–271.

684 Mitchell, A.D., Scholz, A.M., Pursel, V.G. and Evock-Clover, C.M., 1998c. Composition
685 analysis of pork carcasses by dual-energy x-ray absorptiometry. *Journal of Animal*
686 *Science* 76, 2104–2114.

687 National Centre for the Replacement, Refinement and Reduction of Animals in Research
688 2019. The principles of the 3Rs, London, UK.

689 Pomar, C., Rivest, J., Bailleul, P. and Marcoux, M., 2001. Predicting loin-eye area from
690 ultrasound and grading probe measurements of fat and muscle depths in pork
691 carcasses. *Canadian Journal of Animal Science* 81, 429–434.

692 Pomar, C., Kipper, M., Marcoux, M., Pomar, C., Kipper, M. and Marcoux, M., 2017. Use of
693 dual-energy x-ray absorptiometry in non-ruminant nutrition research. *Revista Brasileira*
694 *de Zootecnia* 46, 621–629.

695 R Core Team 2020. R: A language and environment for statistical computing. R Foundation
696 for Statistical Computing, Vienna, Austria. URL <http://www.R-project.org/>.

697 Ruiz-Ascacibar, I., Stoll, P., Bee, G. and Schlegel, P., 2019. Dynamics of the mineral
698 composition and deposition rates in the empty body of entire males, castrates and
699 female pigs. *Animal* 13, 950–958.

700 Ruiz-Ascacibar, I., Stoll, P., Kreuzer, M., Boillat, V., Spring, P. and Bee, G., 2017. Impact of
701 amino acid and CP restriction from 20 to 140 kg BW on performance and dynamics in
702 empty body protein and lipid deposition of entire male, castrated and female pigs.
703 *Animal* 11, 394–404.

704 Schlegel, P. and Gutzwiller, A., 2020. Dietary calcium to digestible phosphorus ratio for
705 optimal growth performance and bone mineralization in growing and finishing pigs.
706 *Animals* 10, 178.

707 Scholz, A.M., Bünger, L., Kongsro, J., Baulain, U. and Mitchell, A.D., 2015. Non-invasive
708 methods for the determination of body and carcass composition in livestock: Dual-

709 energy X-ray absorptiometry, computed tomography, magnetic resonance imaging and
710 ultrasound: Invited review. *Animal* 9, 1250–1264.

711 Soladoye, O.P., López Campos, Ó., Aalhus, J.L., Gariépy, C., Shand, P. and Juárez, M.,
712 2016. Accuracy of dual energy X-ray absorptiometry (DXA) in assessing carcass
713 composition from different pig populations. *Meat Science* 121, 310–316.

714 Speakman, J.R., 1997. Doubly labelled water: Theory and practice. Chapman & Hall,
715 London.

716 Suster, D., Leury, B.J., Ostrowska, E., Butler, K.L., Kerton, D.J., Wark, J.D. and Dunshea,
717 F.R., 2003. Accuracy of dual energy X-ray absorptiometry (DXA), weight and P2 back
718 fat to predict whole body and carcass composition in pigs within and across
719 experiments. *Livestock Production Science* 84, 231–242.

720 Suttle, N., 2010. Mineral nutrition of livestock. CABI, Wallingford, Oxfordshire, UK.

721 Weigand, A.C., Schweizer, H., Knob, D.A. and Scholz, A.M., 2020. Phenotyping of the
722 visceral adipose tissue using dual energy X-ray absorptiometry (DXA) and magnetic
723 resonance imaging (MRI) in pigs. *Animals* 10, 1165.

724 Wickham, H., 2016. ggplot2: Elegant graphics for data analysis. Springer-Verlag, New York.

725
726